Am J Physiol Cell Physiol 292: C1398–C1408, 2006.
First published December 13, 2006; doi:10.1152/ajpcell.00337.2006.

Identification of a putative nuclear localization sequence within ANG II AT_{1A} receptor associated with nuclear activation

Thomas A. Morinelli, John R. Raymond, Aleksander Baldys, Qing Yang, Mi-hye Lee, Louis Luttrell, and Michael E. Ullian

Divisions of Nephrology and Endocrinology, Department of Medicine, Medical University of South Carolina, and the Ralph H. Johnson Veterans Administration Hospital, Charleston, South Carolina

Submitted 19 June 2006; accepted in final form 5 December 2006

Morinelli TA, Raymond JR, Baldys A, Yang Q, Lee M, Luttrell L, Ullian ME. Identification of a putative nuclear localization sequence within ANG II AT_{1A} receptor associated with nuclear activation. *Am J Physiol Cell Physiol* 292: C1398–C1408, 2007. First published December 13, 2006; doi:10.1152/ajpcell.00337.2006.—Angiotensin II (ANG II) type 1 (AT_1) receptors, similar to other G protein-coupled receptors, undergo desensitization and internalization, and potentially nuclear localization, subsequent to agonist interaction. Evidence suggests that the carboxy-terminal tail may be involved in receptor nuclear localization. In the present study, we examined the carboxy-terminal tail of the receptor for specific regions responsible for the nuclear translocation phenomenon and resultant nuclear activation. Human embryonic kidney cells stably expressing either a wild-type AT_{1A} receptor-green fluorescent protein (AT_{1A}R/GFP) construct or a site-directed mutation of a putative nuclear localization sequence (NLS) [K307Q]AT_{1A}R/GFP (KQ/AT_{1A}R/GFP), were examined for differences in receptor nuclear trafficking and nuclear activation. Receptor expression, intracellular signaling, and ANG II-induced internalization of the wild-type/GFP construct and of the KQ/AT_{1A}R/GFP mutant was similar. Laser scanning confocal microscopy showed that in cells expressing the AT_{1A}R/GFP, trafficking of the receptor to the nuclear area and colocalization with lamin B occurred within 30 min of ANG II (100 nM) stimulation, whereas the KQ/AT_{1A}R/GFP mutant failed to demonstrate nuclear localization. Immunoblotting of nuclear lysates with an anti-GFP antibody confirmed these observations. Nuclear localization of the wild-type receptor correlated with increase transcription for both EGR-1 and PTGS-2 genes while the nuclear-deficient KQ/AT_{1A}R/GFP mutant demonstrated increases for only the EGR-1 gene. These results suggest that a NLS (KKFKKY; aa307–312) is located within the cytoplasmic tail of the AT_{1A} receptor and that nuclear localization of the receptor corresponds with specific activation of transcription for the COX-2 gene PTGS-2.

G protein-coupled receptors; cyclooxygenase 2 transcription; laser scanning confocal microscopy

ANGIOTENSIN II (ANG II), a hormone product of the renin-angiotensin system, stimulates both acute and chronic vascular responses producing both physiological and pathophysiological sequelae. Pharmacological and cloning studies have revealed the existence of at least two classes of ANG II receptors, AT_1R and AT_2R. The majority of the physiological, and possibly pathological, events initiated by ANG II are through AT_1R. The AT_1R of mouse and rat is further subdivided into two isoforms, AT_{1A} and AT_{1B}, with 95% homology between the two proteins and significant differences in genomic characteristics, regulation of expression, chromosomal location and tissue distribution. AT_{1A}R is the predominantly expressed isoform, especially in vascular smooth muscle.

Activation by ANG II of AT_1Rs produces G protein-mediated intracellular signals that include activation of tyrosine kinases, nuclear signaling, and vascular remodeling, events which are central to development of atherosclerosis and hypertension (43). Intracellular signaling initiated by ANG II results in AT_1R desensitization and receptor internalization, thus preventing prolonged and recurrent ANG II-induced cellular responses. Internalization of AT_1R occurs by a mechanism that appears to mimic other G protein-coupled receptors (GPCRs) and is similar to that originally described for the β_2-adrenergic receptor. Agonist interaction with the receptor initiates a transition of the receptor from an inactive to an active state and produces activation of the G protein-signaling pathway. Activation of GPCR kinases (GRKs) ensues, producing phosphorylation of residues within the cytoplasmic tail of the receptor with subsequent interaction of the receptor with arrestins. This results in halting further activation of G proteins and directing the receptor to the internalization machinery involving the small GTPase dynamin and clathrin-coated pits. Interestingly, regions of the receptors shown to be involved with the initial activation of specific G proteins may not be the same regions involved in the receptor internalization.

In addition to the plasma membrane-bound AT_1R, cytoplasmic and nuclear ANG II binding sites have been identified (3, 11, 19, 25, 27, 34, 41), as has Ang II-initiated nuclear translocation of an AT_{1A}R/green fluorescent protein (GFP) construct (5). Classically, the sequential movement of proteins into the nucleus is initiated by recognition of the transporting protein, i.e., importin or karyopherin, of the nuclear localization sequence (NLS) of the cargo protein (20). The prototypical NLS, originally identified in the simian virus 40 large t-antigen, constitutes a sequence of basic amino acids, PKKKKKV (29). A common feature of NLSs so far identified is a single sequence of basic amino acids (monopartite) or two clusters of basic amino acids separated by 10–12 residues (bipartite) (7, 20, 29, 35). Although this specific motif is not resident within the AT_{1A}R, regions do exist (residues 307–311) that demonstrate a high concentration of basic residues.

The generation of prostanoids via the activation of the cycloxygenases (COX-1 and COX-2) is responsible for a plethora of both physiological and pathological responses. The activity of constitutive COX-1 results in the generation of prostanoids utilized to maintain physiological homeostasis.

Address for reprint requests and other correspondence: T. A. Morinelli, Division of Nephrology, Dept. of Medicine, 829 Clinical Sciences Bldg., 96 Jonathan Lucas St., Charleston, SC 29425 (e-mail: morinelt@musc.edu).

The costs of publication of this article were defrayed in part by the payment of page charges. The article must therefore be hereby marked "*advertisement*" in accordance with 18 U.S.C. Section 1734 solely to indicate this fact.

The activation of inducible COX-2 has been implicated in numerous pathological events such as rheumatoid arthritis, inflammation, and cancer (38). In vascular smooth muscle, ANG II induces the transcription for COX-2, via involvement of nuclear factor-κB and mediation of several cytoplasmic kinases, including Pyk2, MEKK4, and p38 (6, 21, 31). Thus ANG II is potentially implicated in the activation of several chronic disease processes mediated by COX-2.

Since the original description of resident nuclear receptors for ANG II more than 20 years ago (33), information detailing the trafficking and/or function of nuclear AT_1Rs has not appeared. The present study was designed to address this deficiency. We examined the possibility that the $AT_{1A}R$ possesses a nuclear localization sequence and that nuclear localization of this receptor results in specific nuclear activation. Using human embryonic kidney (HEK-293) cell lines expressing GFP-containing constructs of wild-type or a site-directed mutant of the $AT_{1A}R$, we present findings suggesting that a nuclear localization motif exists at the NH_2-terminal region of the cytoplasmic tail of the $AT_{1A}R$, specifically at lysine^{307} and that nuclear localization of the activated receptor results in the specific induction of the message for COX-2.

EXPERIMENTAL PROCEDURES

Receptor constructs. The cDNA for the rat $AT_{1A}R$ was kindly provided by Dr. Kenneth E. Bernstein, Emory University. The $AT_{1A}R$ expression construct was produced by inserting a coding region of the $AT_{1A}R$ containing a Kozak sequence into the expression vector pcDNA3.1$^+$ (Invitrogen) at *Hind*III/*Xba*I sites. The $AT_{1A}R$-GFP fusion protein expression vector was produced by fusing the coding region of the $AT_{1A}R$ without stop codon to the NH_2-terminus of GFP in frame with the GFP coding sequence at *Xho*I/*Bam*HI sites of pEGFP-N_3 expression vector. The mutation of the $AT_{1A}R$, [K307Q]$AT_{1A}R$, in the $AT_{1A}R$-GFP fusion protein expression vector were generated by using Stratagen's Quick Change Mutagenesis Kit. For construction of the receptor mutant, a PCR primer was designed (cggctttctggggcagaaatttaaaaagtatttcctcc) for the [K307Q]$AT_{1A}R$ mutant. This region of the receptor was chosen for mutation because of its high concentrations of basic lysine residues (KKFKK) mimicking the classic monopartite NLS. Also, others have suggested that this region of the receptor was involved in the nuclear localization phenomenon (27). The PCR products were subcloned into the *Xho*I/*Bam*HI multiple cloning site of the pEGFP-N3 expression vector (enhanced GFP, Clontech). Identities of all constructs were confirmed by sequencing (Medical University of South Carolina Biotechnology Resource Center).

Cell transfections. HEK-293 cells were obtained from American Type Culture Collection and maintained in Ham's F-12 media supplemented with 10% fetal bovine serum (FBS) and penicillin/streptomycin/fungizone. Transfections were carried out using the Lipofectamine 2000 (Invitrogen) transfection reagent according to manufacturer's directions with 10 μg of DNA and 100 μl of lipofectamine in a 100 mm petri dish. Selection of individual stable clones of the transfected HEK cells was performed by exposure of the transfected cells to G-418 (400 μg/ml) 48 h after introduction of the DNA. Individual clones were obtained and maintained in selection media and characterized for $AT_{1A}R$ expression by radioligand binding assays. Individual clones expressing similar levels of AT_{1A} receptors were utilized for all subsequent studies. Cell culture media and supplements were obtained from GIBCO-BRL (Grand Island, NY).

Radioligand binding assays and internalization studies. Binding studies were performed as previously described (5). Confluent monolayers of cells in poly-D-lysine-coated plates (Greiner Bio-One, Longwood, FL) in binding buffer (50 mM Tris, 100 mM NaCl, 5 mM KCl, 5 mM MgCl, 0.25% BSA, and 0.5 mg/ml bacitracin, pH 7.4) were exposed to single concentrations of ANG II (50 fmol of [^{125}I]ANG II; New England Nuclear, Boston, MA) in the presence or absence of unlabeled ANG II (10 μM) for determination of specific binding. Studies were performed at 4°C for 90 min to prevent receptor internalization and thus obtain equilibrium surface binding. Free hormone was removed with three saline washes. Cells were solubilized with 0.1% SDS-0.1 M NaOH, and gamma radioactivity was counted. Specific binding was calculated by subtracting nonspecific binding (<15% of total binding) from total binding. Specific radioactivity bound was corrected for protein content per well and for amount of added [^{125}I]ANG II per well.

For receptor internalization studies, cells were exposed to radioiodinated ANG II at 4°C as described above. Subsequently, cells were either washed with cold saline buffer to remove unbound radioligand and then solubilized as described (*group A*, total receptors available), or acid washed (150 mM NaCl, 50 mM glycine, pH 3.0, for 5 min), solubilized, and associated radioactivity counted (*group B*, nonspecific binding), or washed with cold saline to remove unbound ANG II and then exposed to binding buffer at 37°C for 5 min to allow for internalization, and then acid washed to remove surface-bound radioligand, solubilized, and associated radioactivity determined (*group C*). The amount of internalized receptor was then determined as a percentage from $([C - B]/[A - B]) \times 100$.

Calcium measurements. Individual cell lines were plated into lysine-coated 96-well clear-bottom black plates (Greiner Bio-One, Longwood, FL) at a density of 40,000 cells/well. The next day, media was changed to 0.1% FBS. Forty-eight hours later, cells were incubated with the calcium-sensitive fluorescent probe Fluo-3 AM (2 μM; Molecular Probes) in Hanks' balanced salt solution (HBSS) pH 7.4, containing 2.5 mM Probenecid and 0.1% bovine serum albumin for 60 min, 37°C. At the end of the incubation, the cells were washed 3 times with HBSS and placed into a fluorometric imaging plate reader (FLIPR; Molecular Devices) and exposed to ANG II. A FLIPR is a high-throughput optical screening tool for cell-based fluorometric assays. Increases in intracellular free calcium were reflected by increases in detected fluorescence.

Cell fractionation and immunoblotting. Individual cell lines were plated onto lysine-coated six-well plates (Greiner Bio-One, Longwood, FL) and maintained in selection media until confluence. Medium was changed to 0.1% FBS for 48 h. Medium was then removed and cells washed twice with HBSS (37°C) and then exposed to ANG II (100 nM) or vehicle for the indicated times at 37°C. At the end of the incubation, dishes were placed on ice and gently washed twice with ice-cold phosphate-buffered saline, followed by isolation of cell nuclei using the Subcellular Proteome Extraction kit (Calbiochem, San Diego, CA) according to manufacturer's instructions. Isolated nuclear lysates were concentrated approximately twofold by centrifugation using an Amicon Centricon YM-30 centrifugal filter device (Millipore, Bedford, MA). Concentrated lysates (20–40 μg) were separated by SDS-PAGE (4–20% gradient), transferred to nitrocellulose and probed for the presence of receptor protein using a monoclonal antibody for GFP (BD Biosciences, Palo Alto, CA) or to phosphorylated ERK and total ERK (Cell Signaling Technology, Beverly, MA) according to manufacturers' directions. Detection of protein bands was performed by the addition of CDP-Star reagent (New England Biolabs, Ipswich, MA) and visualized by exposure of the nitrocellulose to radiographic film (X-OMAT, Kodak). Quantitation of the visualized protein bands was performed by densitometric scanning of the exposed radiographic film.

Laser scanning confocal imaging. Individual cell lines were plated onto collagen-coated 25-mm glass coverslips in 6-well plates and maintained in selection medium. Forty-eight hours before the study, the medium was changed to 0.1% FBS. On the day of study, the medium was removed and replaced with HBSS containing 5 μM of the DNA-specific stain DRAQ5 (Alexis, San Diego, CA). Approximately 20 min later, the buffer was removed and the cells were gently

washed twice with HBSS. The coverslip was mounted into a thermoregulated heating block at 37°C (Olympus America, Melville, NY) and HBSS (1 ml) added to the cells. Microscopic images were acquired by using an Olympus microscope UltraView LCI High Resolution workstation (Perkin-Elmer Life Sciences, Boston, MA) equipped with a laser scanning confocal unit (Omnichrome, Chino, CA), 15-mW krypton 3 line laser head, and a UAPO 340 ×40 1.35 or PlanAPO ×60 1.4 numerical aperture oil-immersion objective. GFP fluorescence was excited by using the 488-nm argon laser emission line and collected using a standard fluorescein isothiocyanate filter set (530 ± 30 nm). DRAQ5 was excited with 647-nm krypton laser emission, and images acquired with a 700-nm band-pass filter. Images were analyzed with the proprietary software of the microscope workstation (Ultraview, Olympus America).

For immunofluorescence staining, cells were grown on 35-mm lysine-coated glass-bottom culture dishes (MatTek) and fixed with 4% paraformaldehyde solution in PBS for 15 min at room temperature. Subsequently, the cells were permeabilized with 0.1% Triton X-100 (Sigma) in PBS for 5 min and nonspecific binding sites were blocked with 1% newborn calf serum (Invitrogen) in PBS for 1 h. The cells were then incubated overnight at 4°C with goat polyclonal anti-lamin B (C-20) antibody (1:200) (Santa Cruz Biotechnology), followed by incubation for 1 h at room temperature with Alexa Fluor 555-conjugated secondary antibody (1:200) (Molecular Probes). Confocal microscopy was performed using a laser-scanning microscope (model LSM 510 META, Zeiss) equipped with a ×60 objective, using the following laser wavelengths: excitation 488 nm, emission 505–530 nm and excitation 543 nm, emission 560–615 nm. Three-dimensional visualization of acquired images of *z*-axis scans was performed using Volocity (Improvision, Lexington, MA).

RNA isolation and gene expression profiling. HEK-293 cells were grown to 75% confluence in 6-well plates and serum starved for 16–20 h before stimulation for 90 min with 10 μM of ANG II. After stimulation, cells were harvested, and total cellular RNA was isolated with High Pure RNA Isolation Kit (Roche) according to the manufacturer's protocols. Total RNA (1 μg; A_{260}/A_{280} >2.0) was used for synthesis of cDNA probes. Expression profiles were created using the SuperArray GEArray Q series human G protein-coupled receptor signaling PathwayFinder gene array (HS-008; SuperArray Bioscience, Bethesda, MD). These nylon filter arrays contain 96 known human transcripts specific to GPCR signaling pathways, selected GPCRs, and standardization control markers. cDNA probes were synthesized from purified total RNA using GEarray-specific primers incubated with biotin-16-dUTP, Moloney murine leukemia virus reverse transcriptase, and RNase inhibitor. Gene arrays were prehybridized with sheared salmon sperm DNA before cDNA probe hybridization. Hybridization was done overnight at 60°C for 16 h. Chemiluminescent gene array images were recorded on X-ray film. GEArray Expression Analysis Suite software (Superarray) was used to analyze optimally exposed radiographs. The abundance of each transcript was normalized to housekeeping gene markers on each array.

Real-time quantitative PCR. To quantify the transcription level of EGR-1 and PTGS-2, quantitative real-time PCR was carried out (iCycler iQ Multicolor Real-time Detection System, Bio-Rad). Total RNA was isolated from cells using the High Pure RNA Isolation Kit (Roche). The amount of RNA used for cDNA synthesis was 0.5 μg of total RNA per reaction and iScript cDNA Synthesis Kit (Bio-Rad) was used making cDNAs. cDNA was amplified with the PCR (GENIUS, 25°C for 5 min, 42°C for 30 min, 80°C for 5 min; one cycle) using primers containing the oligo (dT) and random hexamer DNA sequence. The amplified cDNAs were used as template DNAs for quantitative real-time PCR. Reagent (iQ SYBR Green Supermix) was obtained from the same supplier (Bio-Rad) and used as described by manufacturer. The primer sets were designed to span the intron-exon borders to distinguish amplified cDNA from genomic DNA. Specific primer pairs used for amplification were the following: EGR1 sense, 5′-GATGATGCTGTGACAATAAG-3′, EGR1 anti-sense 5′-TACGGTCAAGCAGTATTTAC-3′ and PTGS-2, sense 5′-TTCTCTAACCTCTCCTATTATAC-3′ and PTGS-2, anti-sense 5′-TTCCACAATCTCATTTGAATC-3′. Serial dilutions of a template cDNA that isolated from AT_1-wild-type transfected cells with 10 μM of ANG II stimulation for 90 min were made for PCRs to optimize the PCR products within the linear range. The conditions for the PCR reactions were the following: denaturation at 95°C for 10 s and annealing at 51°C for 45 s for 40 cycles. The data were analyzed using the iCycler software and Excel. The expression level of EGR1 and PTGS2 from each samples were normalized using the mRNA expression levels of the housekeeping gene GAPDH.

Statistics. Means ± SE from the indicated number of studies (*n*) were compared using Microsoft Excel. Tests for significance were done using a Student's *t*-test when comparing two sets of data or by ANOVA with Fisher's post hoc *t*-test when three or more comparisons were made. Significant differences were indicated at the 95% level.

RESULTS

For visualization of receptor trafficking to the nucleus, as well as determining receptor sequence(s) required for this translocation, GFP constructs of the wild-type $AT_{1A}R$ and a site-directed mutant were made. In an effort to identify a nuclear localization motif in the $AT_{1A}R$, a single point substitution of a glutamine for lysine at position 307, the putative nuclear localization motif was constructed, [K307Q]$AT_{1A}R$/GFP. This region of the carboxy-terminal tail of the receptor contains a series of positively charged residues (KKFKK) mimicking the classic NLS, and also has been suggested to be involved in the nuclear localization phenomenon (27).

The HEK-293 cell line has been used extensively as a model cell for investigations into the signal transduction pathway for $AT_{1A}Rs$ (14, 28, 44, 45). Through G-418 resistance, stable clones for each receptor construct were obtained. Receptor expression was characterized through laser scanning confocal microscopy (LSCM), immunoblotting with an antibody to GFP, and screened by ANG II radioligand binding and functional responsiveness to ANG II. Images obtained from LSCM demonstrated membrane-associated fluorescence in the two cell lines expressing the $AT_{1A}R$ constructs, indicating membrane localization of the receptor. In certain cells, aggregated fluorescence is seen in the perinuclear region of the golgi bodies (Fig. 1, *B* and *C*). In the cells expressing only GFP, fluorescence was seen dispersed throughout the cells (Fig. 1*A*). Immunodetection using a monoclonal antibody to GFP of total cell lysates from HEK cells expressing the wild-type $AT_{1A}R$/GFP construct identified the $AT_{1A}R$/GFP receptor at an approximate molecular size of 79 kDa (Fig. 1*D*). This band was not seen in the cells expressing only GFP.

Through equilibrium radioligand binding assays, cell lines expressing similar levels of the $AT_{1A}R$ constructs were obtained (Fig. 1*E*). Cells transfected with GFP alone did not demonstrate specific binding of [^{125}I]ANG II. To demonstrate that the expressed $AT_{1A}R$ constructs produced a functional response in the HEK cell lines, we measured elevations in intracellular free calcium using the calcium-sensitive fluorescent dye fluo-3. HEK cells stably expressing each of the $AT_{1A}R$/GFP constructs as well as the nonfluourescent wild-type $AT_{1A}R$ responded in a concentration-dependent manner to the addition of ANG II (Fig. 2*A*). Cells expressing GFP only did not respond to addition of ANG II. Pretreatment of the cells with an excess of the specific AT_1R antagonist losartan (10 μM

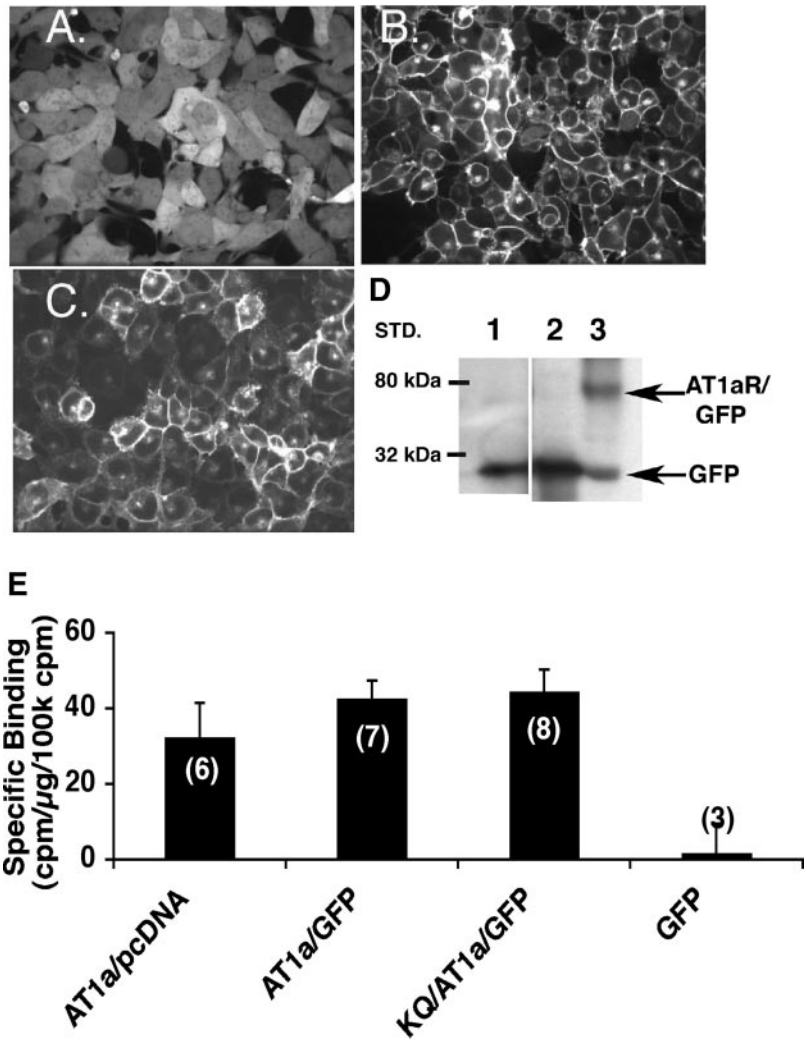

Fig. 1. Characterization of stably expressed angiotensin type 1A receptor ($AT_{1A}R$)/green fluorescent protein (GFP) constructs. Laser scanning confocal microscope (LSCM) images of GFP/human embryonic kidney (HEK) cells (*A*), $AT_{1A}R$/GFP/HEK cells (*B*), and [K307Q]$AT_{1A}R$/GFP/HEK cells (*C*). *D*: GFP immunoblot of *1*) recombinant GFP (5 ng), *2*) GFP/HEK cell lysate (5 μg), and *3*) $AT1_AR$/GFP/HEK cell lysate (5 μg). Position of bands shown by arrows indicates location of $AT_{1A}R$/GFP and of GFP. STD, standard. *E*: surface expression of AT_{1A} receptors in HEK cell lines stably expressing the $AT_{1A}R$ constructs. Cells were assessed for expression of $AT_{1A}Rs$ through equilibrium radioligand binding assays using [^{125}I]ANG II as described. $AT_{1A}R$ in pcDNA3.1 (AT_{1A}/pcDNA); wild-type $AT_{1A}R$/GFP (AT_{1A}/GFP); [K307Q]/$AT_{1A}R$/GFP (KQ/AT_{1A}/GFP) and GFP alone expressing cells (GFP). Values shown are the average (±SE) from indicated number of studies (*n*).

and 100 μM) for 5 min significantly inhibited the responses (Fig. 2*B*), indicating mediation of the AT_1R. The EC_{50} values for each cell line and the maximum stimulated response (Table 1) for the various cell lines were not significantly different. Interaction of ANG II with the AT_1R initiates activation of several kinase pathways, including that for extracellular-regulated kinase (ERK, p42/44). Phosphorylation and activation of ERK results in nuclear localization of the activated enzyme. The addition of ANG II to HEK-293 cells stably expressing either the wild type $AT_{1A}R$/GFP or the KQ/$AT_{1A}R$/GFP resulted in a time-dependent increase in nuclear localization of phosphorylated ERK (Fig. 3). There was no significant difference in the time course for the localization of the activated ERK between cells expressing the wild-type receptor and the putative NLS-deficient receptor (Fig. 3*B*).

Interaction of the $AT_{1A}R$ with its cognate ligand ANG II results in the rapid internalization of the receptor-ligand complex, a common feature of many GPCRs. In HEK cells stably expressing either wild-type $AT_{1A}R$/GFP or the [K307Q]$AT_{1A}R$/GFP mutant receptor (putative NLS-deficient mutant), similar internalization dynamics were seen. Five minutes exposure of the cells at 37°C resulted in 63% ± 9% (n = 4) and 57% ± 14% (n = 5) internalization of surface $AT_{1A}Rs$ for the wild-type and KQ/$AT_{1A}R$/GFP receptors, respectively. Thus, both receptor constructs demonstrate similar surface receptor expression, intracellular signaling, and receptor internalization dynamics.

Having demonstrated similar receptor expression and function, we then determined whether the mutant receptor differed in its ability to localize to the nucleus. Using LSCM and the HEK cell line expressing the wild-type $AT_{1A}R$/GFP, with DRAQ5 nuclear staining, we demonstrated receptor internalization and localization to the nucleus in a time-dependent manner, subsequent to ANG II stimulation. The wild-type receptor was seen to internalize, evidenced by cytoplasmic "speckling", and by 30-min post-ANG II exposure, co-localizing to the nucleus, as evidenced by the presence of "yellow" over the nuclear area (Fig. 4). Cells expressing the KQ/$AT_{1A}R$/GFP mutant did not demonstrate an increase in intensity within the nuclear area subsequent to ANG II stimulation. Receptor internalization, indicated by the cytoplasmic "speckling" was seen in these cells (Fig. 4), with aggregation of the internalized receptor near the nuclear area. These data, acquired from live cells visualized in two-dimensions, appeared to indicate the nuclear localization of the wild-type $AT_{1A}R$. In additional studies, a more detailed analysis of this response, using z-axis scanning with subsequent three-dimensional rendering with Volocity software, showed that the wild-type receptor appeared to localize to the nuclear membrane subsequent to 60

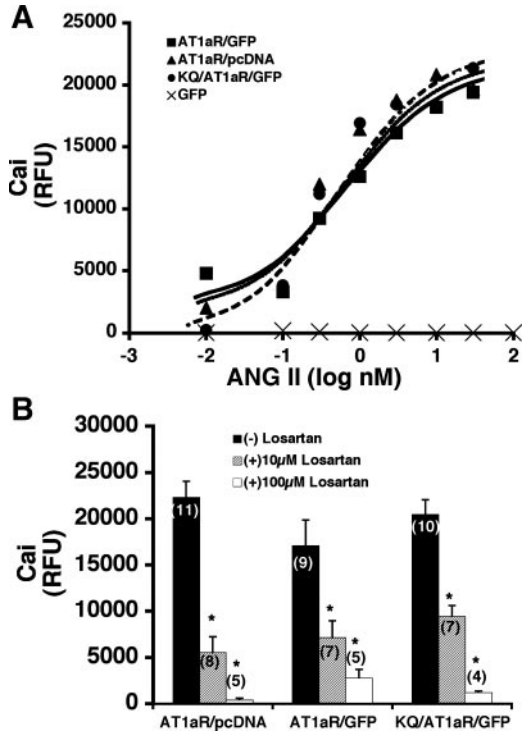

Fig. 2. ANG II-stimulated increases in intracellular free calcium in HEK-293 cells expressing the $AT_{1A}R$ constructs. *A*: concentration-response curves for ANG II-induced elevations in intracellular free calcium (Ca_i). Individual HEK-293 cell lines were loaded with the intracellular fluorescent calcium probe Fluo-3 and exposed to the indicated concentrations of ANG II. Values are from a single study done in triplicate and are representative of 5–11 similar studies. RFU, relative fluorescence units. *B*: maximum fluorescence stimulated by ANG II (100 nM) in the absence or presence of the AT_1R antagonist losartan is shown for each cell line. Average values from indicated number of studies (*n*) performed in triplicate. $*P < 0.05$ vs. ANG II alone for each cell line.

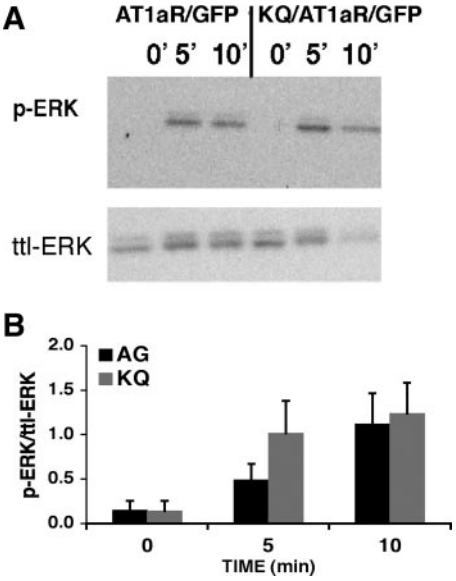

Fig. 3. ANG II-induced nuclear localization of phosphorylated ERK. *A*: representative immunoblot of 3 similar studies. *B*: summary of densitometric scans of immunoblots. Amount of phospho-ERK (p-ERK) was corrected for amount of total ERK (ttl-ERK) in the nuclear lysates from the two cells lines at each time point (AG, $AT_{1A}R$/GFP; KQ, [K307Q]/$AT_{1A}R$/GFP). HEK-293 cells stably expressing the indicated $AT_{1A}R$ constructs were exposed to 100 nM ANG II for the indicated periods of time. Nuclear extracts (20 μg) were prepared, separated by SDS-PAGE, transferred to nitrocellulose, and immunoblotted with an antibody to activated ERK (p-ERK). Blots were subsequently stripped and reprobed with an antibody to total ERK. AT_{1A}, $AT_{1A}R$/GFP; KQ, [K307Q]/$AT_{1A}R$/GFP. Values shown are the average from 3 similar studies (±SE).

min of stimulation by ANG II. Receptor localization to the nucleus appeared as aggregated speckling at the nuclear surface (Fig. 5*A*), with the "green" receptor intercalating into the "red" of the nucleus, i.e., localizing with the DNA dye DRAQ5. Volocity software allows for alterations in voxel (volume pixels) opacity, or density, when performing three-dimensional rendering. When the opacity is set at 100% the voxels from the red or nuclear DNA/DRAQ5 channel appear as solid nuclei with the green receptor at its surface for the wild-type-expressing cells (Fig. 5*A*) and aggregated in a peri-nuclear region for the cells expressing the K307Q mutant receptor. However, when the opacity of the red voxels was reduced to 50%, allowing for visualization through the surface of the nucleus, surface localization was seen as being integrated into the nuclear area for the wild-type receptor, as indicated by the "yellow" in Fig. 5*C*.

Table 1. *Comparison of ANG II-stimulated increases in intracellular free calcium in various stable HEK-293 cell lines*

	$AT_{1A}R$/pCDNA3.1	$AT_{1A}R$/GFP	KQ/$AT_{1A}R$/GFP
EC_{50}, nM	0.29±0.09	0.12±0.07	0.16±0.05
MAX, RFU	22,286±1,764	17,078±2,759	20,457±3,261
	n = 11	*n* = 9	*n* = 10

Values are means ± SE; *n,* no. of studies. HEK, human embryonic kidney; GFP, green fluorescent protein; $AT_{1A}R$, ANG type 1A receptor; EC_{50}, concentration of ANG II producing a half-maximal response; MAX, maximum fluorescence produced by 100 nM ANG II; RFU, relative fluorescence units as an indicator of intracellular free calcium.

Having seen that the wild-type receptor integrates into the nuclear area with the DRAQ5/DNA dye, we next examined the relationship of the receptor with the nuclear envelope itself. For these studies, cells expressing either the wild-type $AT_{1A}R$/GFP or the K307Q/$AT_{1A}R$/GFP constructs were exposed to ANG II for 60 min, followed by paraformaldehyde fixation and immunofluorescence staining with an antibody to lamin-B, a structural component of the nuclear membrane. Unstimulated HEK cells expressing the $AT_{1A}R$/GFP construct demonstrated plasma membrane distribution of the receptor and no colocalization with lamin B, indicating a lack of association of the receptor with the nuclear envelope in the basal state (Fig. 6, *A* and *B*). Similar distribution of the receptor was seen with unstimulated cells expressing the K307Q/$AT_{1A}R$/GFP construct (data not shown). After exposure of the cells expressing the wild-type receptor to ANG II for 60 min, the internalized receptor colocalized with lamin B and in the three-dimensional reconstruction, appears inserted within the lamin B staining (Fig. 6, *C* and *D*). However, in cells expressing the NLS-deficient mutant, the internalized receptor is once again seen to concentrate in a peri-nuclear region (Fig. 6, *E* and *F*). Cells expressing GFP alone do not show any colocalization or changes in distribution of GFP after exposure to ANG II (Fig. 6, *G* and F). These images indicate that the nuclear

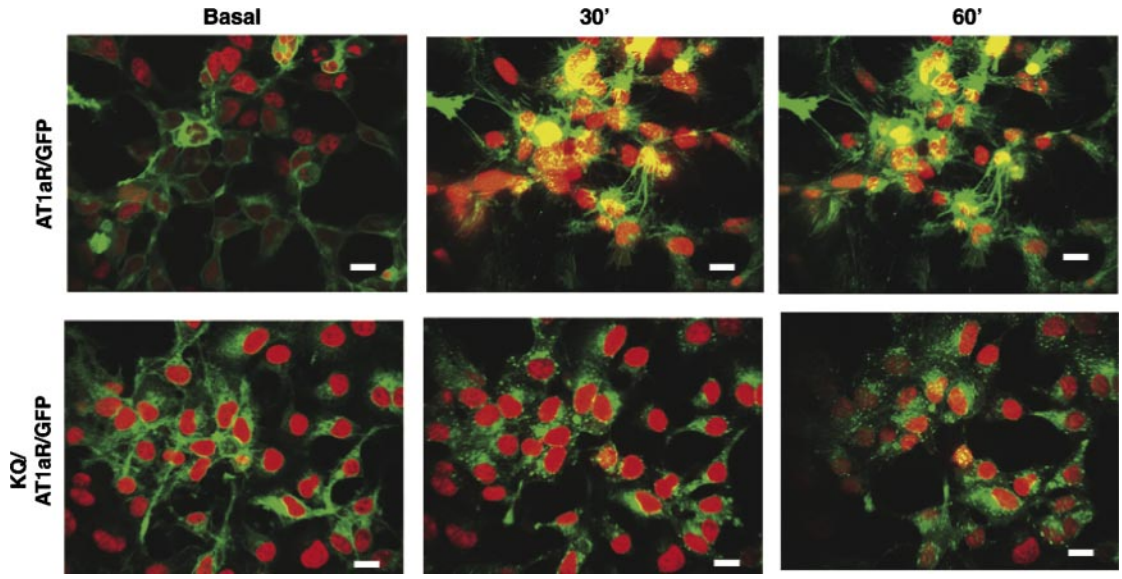

Fig. 4. Laser scanning confocal microscopy (LSCM) images of live cells showing the effects of ANG II stimulation on nuclear localization of the $AT_{1A}R$/GFP constructs. HEK-293 cell lines stably expressing the wild-type receptor, $AT_{1A}R$/GFP, or the [K307Q]$AT_{1A}R$/GFP mutant receptor (KQ/$AT_{1A}R$/GFP) were exposed to ANG II (100 nM, 37°C) and time-lapsed images were acquired for up to 60 min (minute shown as ′ symbol) post-ANG II addition. Images shown are from the indicated cell lines taken before exposure to ANG II (Basal) and at 30 min and 60 min post-ANG II addition. Nuclei are shown by staining with the DNA specific fluorescent dye DRAQ5 (red). Receptors are indicated as green. Nuclear localization of the wild-type receptor is shown in yellow. Images acquired as described using a ×40 objective. Images shown are representative from five similar studies. Scale bar indicates 10 μm.

localization of the wild-type receptor after exposure of the cells to ANG II appears to be the result of colocalizing with the nuclear membrane. The nuclear localization response of the wild-type receptor was also observed in additional stable cell lines expressing threefold lower levels of the $AT_{1A}R$/GFP, as determined by radioligand binding assays (data not shown).

These observational studies utilizing the LSCM were confirmed through immunoblotting of nuclear extracts from cells stimulated by ANG II. $AT_{1A}R$/GFP-expressing HEK cells, when stimulated by ANG II (100 nM) for 30 min, demonstrated an approximate twofold increase in $AT_{1A}R$/GFP expression in nuclear extracts as demonstrated by anti-GFP immunoblotting (Fig. 7). This increase was inhibited by preincubation with the specific AT_1R antagonist losartan (10 μM). Receptor localization to the nucleus was not seen in ANG II-stimulated HEK cells expressing the KQ/$AT_{1A}R$/GFP mutant (Fig. 7). The purity of the nuclear fractions obtained was confirmed by immunoblotting studies using antibodies for calpain (cytoplasmic marker), the transcription factor CREB

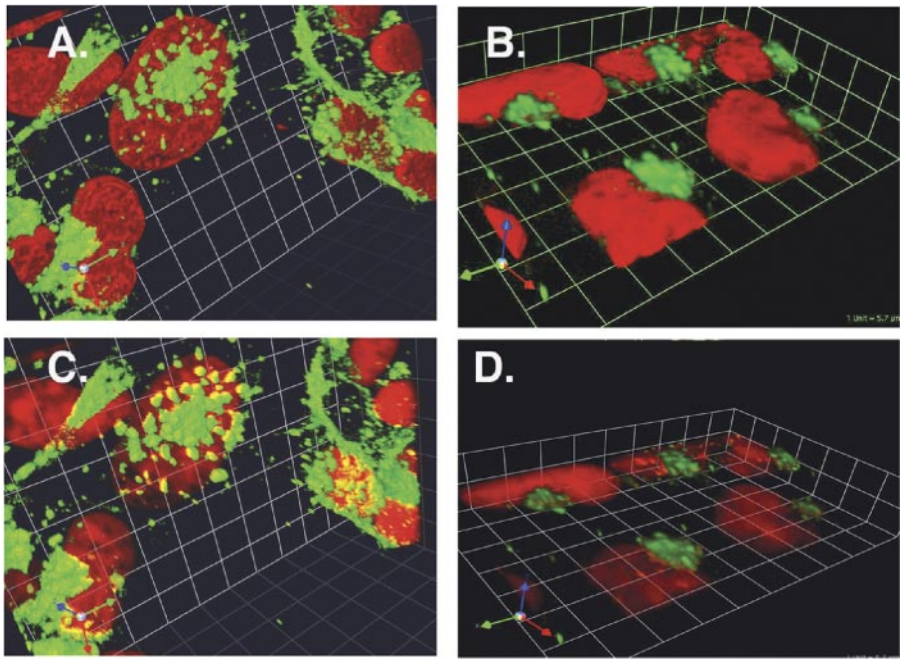

Fig. 5. Three-dimensional visualization of $AT_{1A}R$/GFP trafficking. HEK-293 cells stably expressing the wild-type $AT_{1A}R$/GFP construct (*A* and *C*) or the nuclear localization sequence (NLS)-deficient mutant KQ/$AT_{1A}R$/GFP (*B* and *D*) were exposed to ANG II (100 nM) for 60 min. Images were acquired through *z*-axis scanning with subsequent three-dimensional rendering using Volocity software (Improvision). Nuclei are indicated by staining with DRAQ5 (red) and are shown at a density of 100% (*A* and *B*) or 50% (*C* and *D*). Calibration grid is 5 μm/U. Representative images from three similar studies using a ×40 objective as described.

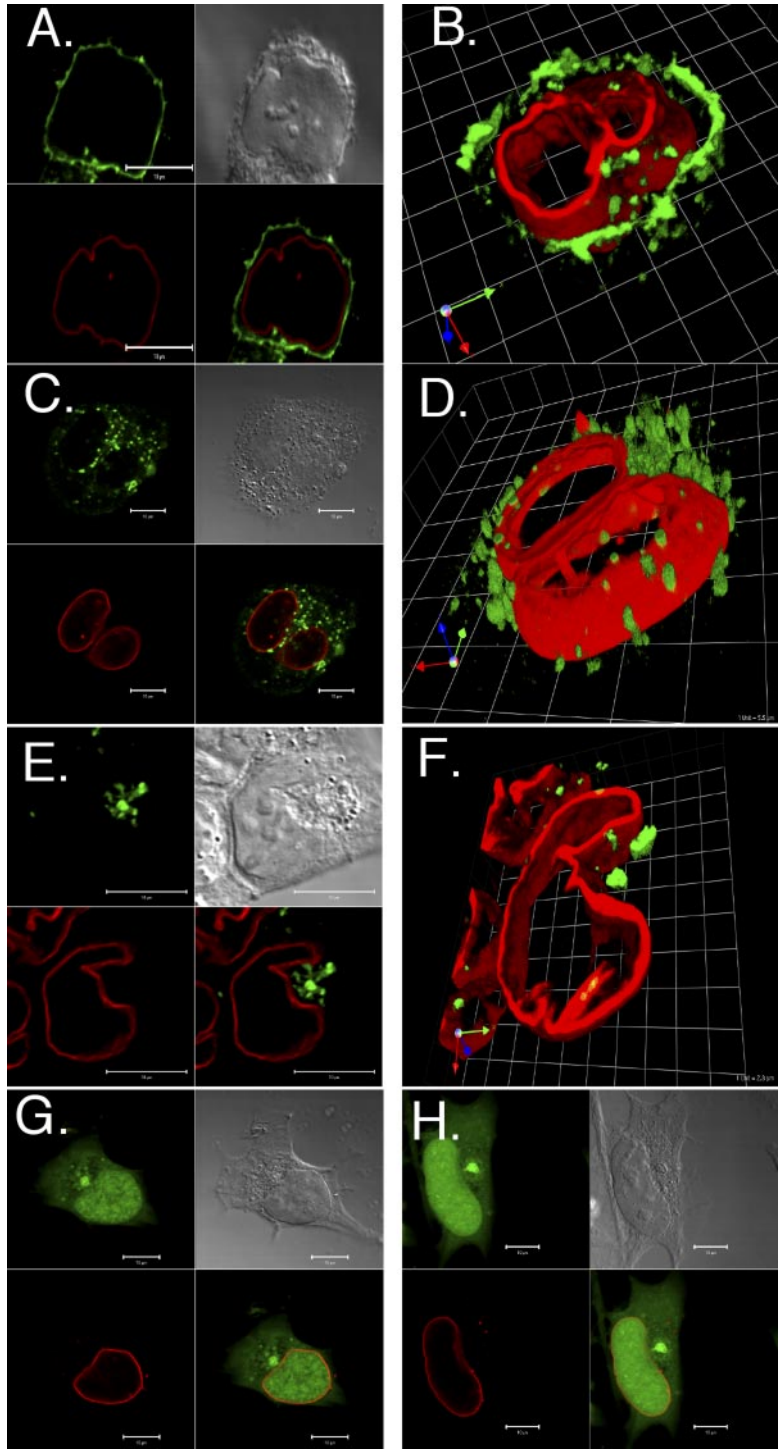

Fig. 6. Confocal laser scanning microscopic images of colocalization of $AT_{1A}R$/GFP with lamin B. HEK-293 cells stably expressing either the wild-type $AT_{1A}R$ or the NLS-deficient K307Q mutant were exposed to ANG II (100 nM) for 60 min and prepared for immunofluorescent staining of the nuclear envelope protein lamin B as described. Images shown demonstrate location of the receptor/GFP constructs (green) and of lamin B (red) as well as phase contrast images and three-dimensional reconstruction of *z*-axis scans through a portion of the cells (*B*, *D*, and *F*). Cells are from unstimulated $AT_{1A}R$/GFP/HEK cells (*A* and *B*), $AT_{1A}R$/GFP cells exposed to ANG II (*C* and *D*), K307Q/$AT_{1A}R$/GFP/HEK cells exposed to ANG II (*E* and *F*), and GFP/HEK cells unstimulated (*G*) and exposed to ANG II (100 nM) for 60 min (*H*). Scale bar indicates 10 μm.

(nuclear marker), and sodium/potassium ATPase, a marker for plasma membrane (Fig. 7*C*).

To determine the consequences of the nuclear localization of the $AT_{1A}R$ we examined nuclear activation of transcription through the use of DNA arrays and real-time PCR. A commercially available human G protein-coupled receptor signaling PathwayFinder gene array, expressing 96 different genes, was used to compare DNA expression by wild-type $AT_{1A}R$ and the nuclear localization-deficient KQ mutant. HEK cells stably expressing the wild-type $AT_{1A}R$/GFP construct, when exposed to ANG II (10 μM, 90 min), demonstrated significant increases in the expression of two genes, early growth response gene-1 (Egr-1) and the gene for cyclooxygenase-2 (COX-2), PTGS-2. Cells stably expressing the nuclear-localization deficient construct KQ/$AT_{1A}R$/GFP showed a significant increase in only the Egr-1 gene and not that for COX-2 (Fig. 8). These findings were confirmed through the utilization of quantitative real-time PCR (Fig. 9), thus showing that nuclear localization of the ANG II $AT_{1A}R$ is necessary for activation of the COX-2 gene.

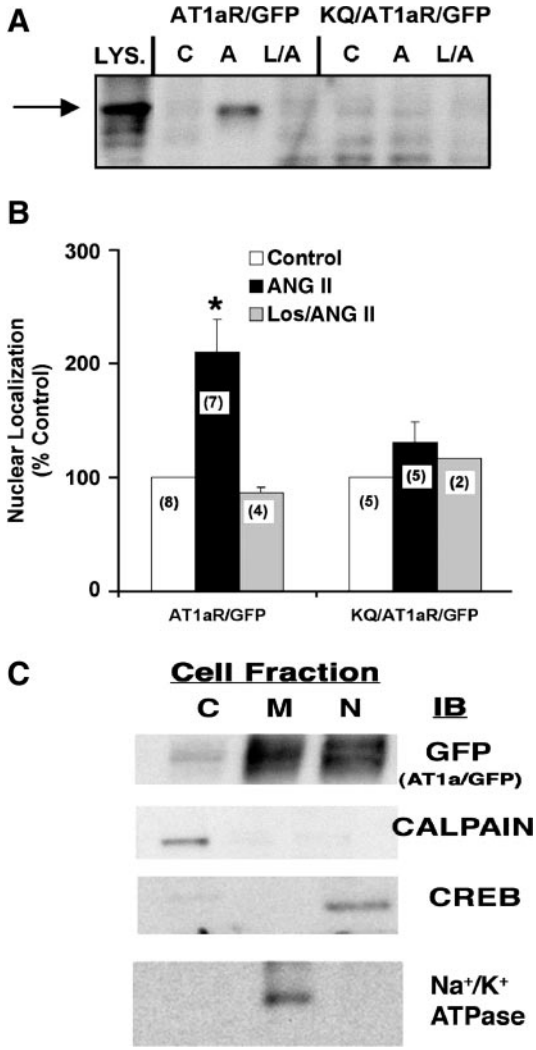

Fig. 7. Immunoblot analysis of $AT_{1A}R$/GFP nuclear localization. HEK-293 cells stably expressing either the wild-type receptor, $AT_{1A}R$/GFP or the NLS-deficient receptor [K307Q]$AT_{1A}R$/GFP (KQ/$AT_{1A}R$/GFP) mutant constructs were exposed to buffer or losartan (10 μM, 15 min), followed by ANG II (100 nM, 30 min). Nuclear lysates were prepared as described and proteins (20 μg) separated by SDS-PAGE, transferred to nitrocellulose and probed with a monoclonal antibody to GFP (BD Biosciences). *A*: representative study showing nuclear expression of the receptor/GFP constructs from the two cell lines after exposure to vehicle (C) or ANG II (A) or to losartan and ANG II (L/A). Whole cell lysate (LYS) of cells expressing the wild-type $AT_{1A}R$/GFP receptor is shown to identify location of the $AT_{1A}R$, indicated by arrow. *B*: summary of scanning densitometry of the obtained immunoblots showing changes in protein density in samples stimulated by ANG II compared with control, unstimulated samples and samples preexposed to the AT_1R antagonist losartan. Average values from the indicated number of studies (n ± SE). *C*: representative immunoblots of cytosolic (C), membrane (M) and nuclear (N) fractions from unstimulated $AT_{1A}R$/GFP/HEK cells probed with antibodies to GFP, calpain (cytosolic protein), CREB (nuclear protein), and Na^+-K^+-ATPase (membrane protein) indicated on right, demonstrating purity of the individual cell fractions used in these studies. *$P <$ 0.05 vs. control and Los/ANG II.

DISCUSSION

The data presented in the current study demonstrates the following: *1*) characterization of a wild-type AT_{1A}/GFP receptor and a site-directed receptor mutant stably expressed in HEK-293 cells, *2*) mutation of a single lysine residue, lysine[307], produced loss of receptor nuclear localization without altering receptor internalization or intracellular signaling, *3*) nuclear localization appears to involve the nuclear envelope protein lamin B, and *4*) nuclear localization of the $AT_{1A}R$ is associated with activation of the gene for COX-2 in response to Ang II stimulation.

Initiation of GPCR trafficking results from the interaction of cognate ligands with their endogenous receptors, producing activation of intracellular kinases and phosphorylation of numerous specific and kinase-dependent target proteins, including the receptor itself. Phosphorylation of specific residues by kinases results in the desensitization and internalization of the receptor. In the case of $AT_{1A}Rs$, receptor-induced activation of G protein-coupled receptor kinases (GRKs) produces phosphorylation of specific residues on the cytoplasmic tail of the AT_{1A} receptor. Regions within the AT1R have been identified as being essential for internalization of the activated receptor. One region of the receptor demonstrated to be required for endocytosis is amino acids 331–338 (-STKMSTLS-) located within the cytoplasmic tail of the receptor (22, 40, 42). Additional residues within the cytoplasmic tail of the receptor have been identified as critical for internalization including leucine[316] and tyrosine[319] (42). Substitution of asparagine or alanine for methionine[134], or replacement of the highly conserved residues asparagine[125] and arginine[126] with alanine, both within the second intracellular loop, results in loss of internalization and intracellular and nuclear signaling (13). Analogous to other GPCRs, the AT_1R contains an $NPX_{2-3}Y$ sequence, which in the $AT_{1A}R$ is located at residues 298–302 (NPLFY). This sequence has been demonstrated in other GPCRs to be involved in receptor internalization (1). Interestingly, with the $AT_{1A}R$, this is not the case. Mutations in this region do not alter internalization dynamics (23, 42).

Since the early 1980s, evidence has gradually accumulated regarding the existence of nuclear Ang II binding sites. The earliest studies showed specific Ang II activation of RNA synthesis in isolated hepatic nuclei (33). Two more detailed pharmacological approaches demonstrated specific ANG II binding sites in membranes of isolated hepatic nuclei. These studies showed that although the receptors associated with the nuclear membranes were similar in their binding characteristics and their ability to show decreased receptor affinity in the presence of nonhydrolyzable GTP analogues, their physiochemical properties differed from those found in the plasma membrane in that the binding sites found in the nuclear membranes appeared to be soluble proteins (3, 41). A subsequent study demonstrated that nuclear ANG II "receptors" are capable of not only interacting with ANG II, but also initiating nuclear responses. The addition of ANG II to isolated hepatic nuclei specifically increased the transcription of RNA for renin and angiotensinogen (9). Further pharmacological analysis of the ANG II nuclear "binding sites" indicated that these sites could be classified as ANG II AT_1Rs and that they mediated the ANG II-induced transcription for growth factors, such as platelet-derived growth factor, and for renin and angiotensinogen as well (10). Cytoplasmic injection of ANG II has also elicited both cytoplasmic and nuclear responses including elevations in intracellular free calcium and tritiated thymidine incorporation, respectively (11, 12). Finally, a intracellular renin-angiotensin system has been suggested to exist with the demonstration through utilization of immunofluorescence and

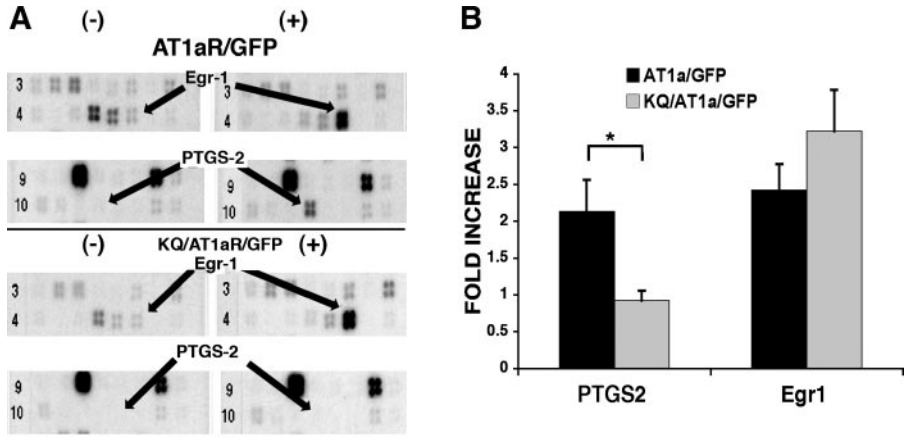

Fig. 8. ANG II-induced activation of gene expression. HEK-293 cells stably expressing either the wild-type $AT_{1A}R$/GFP or the KQ/$AT_{1A}R$/GFP construct were exposed to vehicle or to ANG II (10 μM, 90′), RNA isolated, cDNA transcribed and hybridized to the membranes as described. Chemiluminescent detection and *s*canning densitometry was used to quantitate differences in gene expression between cells exposed to vehicle and those exposed to ANG II in the two different cell lines. *A*: representative blots from each cell line exposed to vehicle (−) or to ANG II (+). *B*: summary of densitometric scanning of the changes in gene expression for early growth response (EGR)-1 and for PTGS-2 compared with unstimulated cells from the obtained blots (average ± SE, $n = 4$, $^*P < 0.05$, locus of gene indicated).

confocal microscopy, of nuclear ANG II and ANG 1–7 in mesangial cells (4).

Activation of cell surface AT_1Rs generates intracellular signals that result in nuclear translocation of second messengers (MAPK, STAT) (2, 8, 18, 30), initiating nuclear events, such as activation of transcription factors, specific DNA binding proteins, and protein synthesis (2, 13, 16, 36, 43). ANG II activates several proto-oncogenes involved in cell proliferation including the early growth response gene (Egr-1) (17, 26, 37).

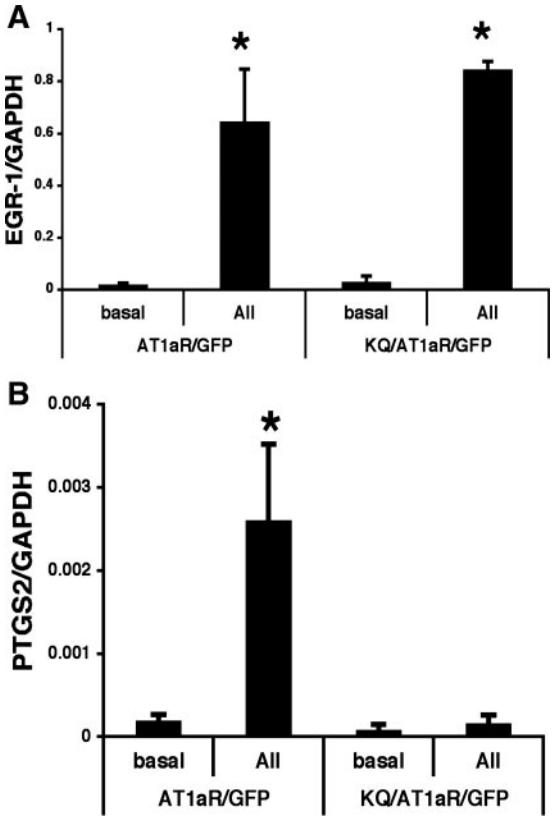

Fig. 9. Real-time PCR analysis of Egr-1 and PTGS-2 gene induction. Cells stably expressing either the wild-type $AT_{1A}R$/GFP (AG) or the nuclear localization-deficient mutant [K307Q]/$AT_{1A}R$/GFP (KQ/AT1A/GFP), were exposed to vehicle or to ANG II (AII, 10 μM, 90′). RNA was isolated, cDNA prepared, and PCR performed as described. Number of cycles to reach threshold was determined for each gene and compared with that for GAPDH for each treatment. Average values ± SE from 3 similar studies, $^*P < 0.05$.

Egr-1, a member of the family of zinc finger transcription factors, regulates cell cycle progression (15) and has been shown to mediate the ANG II activation of cyclin D1 (17).

COX-2, a product of the PTGS-2 gene, and an enzyme responsible for metabolizing arachidonic acid into prostaglandin G2 (PGG2), has been implicated in several pathologies, including pain, inflammation, and cancer. COX-2 activity may also be responsible for normal kidney development (38). ANG II alters the expression for PTGS-2 and COX-2. Indeed, in vascular smooth muscle cells, the increase in message for COX-2 is mediated by activation of intracellular kinases, resulting in an increased message half-life and increased protein expression (6, 21, 31). Alternatively, as in our studies, trafficking of the AT_1R itself into the nucleus, or nuclear membrane, may be a stimulus for initiating PTGS-2 expression. How nuclear membrane localization of the $AT_{1A}R$ results in activation of the PTGS-2 gene is not yet understood. However, several possible mechanisms for this effect may be derived from nuclear trafficking of other receptors and signaling molecules. Recently, activation of the δ-opioid receptor was shown to promote nuclear translocation of β-arrestin 1 and subsequent association with the promoter regions of p27 and c-fos (24). Pokholok et al. (32), demonstrated the association of mitogen activated kinases with genes whose expression has been shown to be under the control of those kinases. p38, a member of the MAPK family and mediator of ANG II-induced expression of COX-2 in vascular smooth muscle cells, was shown to directly phosphorylate transcription factors during myogenesis (39). The $AT_{1A}R$, as described above, when activated, associates with β-arrestin 1 and is subsequently internalized. Thus as the receptor is localized to the nuclear envelope it may act as a scaffold for the translocation of β-arrestin 1, p38, or other, as yet unidentified proteins, for the purpose of delivering these proteins to the nucleus for activation of the PTGS-2 gene. It should also be noted that although our data show a lack of both nuclear localization and activation of the PTGS-2 gene by the NLS-deficient $AT_{1A}R$, these two phenomena may not be directly linked. Other alterations in signaling other than those that were examined in this study may exist for the mutant receptor causing the loss of PTGS-2 gene induction.

In addition to our present data, Lu et al. (27) demonstrated nuclear translocation of the AT_1R in response to cellular activation by ANG II. This group, using indirect methods of immunofluoresent staining and immunoblotting, demonstrated

an increase in immunoreactivity of the AT_1R in nuclei of cultured neuronal cells subsequent to stimulation by ANG II. This effect was both time and concentration dependent and was inhibited both by losartan, an AT_1R-specific antagonist and by a synthetic peptide corresponding to residues 295–315 of the carboxy-terminal tail of the $AT_{1A}R$. The trafficking of the receptor to the nucleus seen in this study, appeared to correlate with phosphorylation of p62 nucleoporin, a component of the nuclear pore complex, thus suggesting involvement of the complex with the nuclear localization of the receptor. Lee et al. (25), using GFP receptor constructs, demonstrated nuclear localization of not only the AT_1R but also of the bradykinin B_2 and apelin receptors. Interestingly, this group showed that the nuclear localization of these receptors occurred in the absence of agonist stimulation and was cell specific. The apelin receptor localized to the nucleus only in neuronal cells and not in HEK-293 cells. The AT_1R and B2 receptors demonstrated nuclear localization in the HEK-293 cell line. An examination of the amino acid sequence of the bradykinin B2 and apelin receptor indicates that the cytoplasmic tails of these receptors do not possess an area of concentrated lysine residues, like that for the $AT_{1A}R$. However, this region of the B2 receptor does contain a high concentration of basic residues, i.e., KRFRK, which can also act as a NLS. Interestingly, the apelin receptor demonstrates an area of basic residues in the third cytoplasmic loop, i.e., RKRRR. In the study by Lee et al., mutation in this region of the apelin receptor prevented nuclear localization of the receptor in the neuronal cell line. The fact that the nuclear localization of the apelin receptor appeared to be cell specific may be the consequence of this difference in location of the putative NLS seen between the AT1R, the B2 receptor and the apelin receptor.

In our current studies, a single point mutation of lysine^{307} to glutamine produced an $AT_{1A}R$, which recognized ANG II, internalized subsequent to binding ANG II, transduced a calcium signal in response to ANG II, and generated nuclear localization of phosphorylated ERK, but failed to localize to the nucleus and failed to activate the PTGS-2 gene. In addition, whereas previous studies have shown localization of certain GPCRs to the nuclear area, raising the question of how a membrane-bound receptor could function in the nucleoplasm, our present study shows receptor colocalization with lamin B, a structural component of the nuclear envelope. As such, this provides evidence that an integral plasma membrane receptor can localize to the nuclear membrane and maintain its physical-chemical properties of a membrane bound protein. Future studies will determine the mechanism for the nuclear import of the $AT_{1A}R$.

ACKNOWLEDGMENTS

We thank Katie Blake and Jana Fine for providing extensive technical expertise. A portion of this work was presented at the American Society of Nephrology Meeting, November 8–13, 2005, Philadelphia, PA.

GRANTS

This work was supported from research awards from Dialysis Clinic Incorporated and the Department of Veterans Affairs shared equipment grant and the Research Enhancement Award Program from the Department of Veterans Affairs.

REFERENCES

1. **Barak LS, Tiberi M, Freedman NJ, Kwatra MM, Lefkowitz RJ, Caron MG.** A highly conserved tryosine residue in G protein-coupled receptors is required for agonist-mediated β2-adrenergic receptor sequestration. *J Biol Chem* 269: 2790–2795, 1994.
2. **Bhat G, Thekkumkara T, Thomas W, Conrad K, Baker K.** Angiotensin II stimulates sis-inducing factor-like DNA binding activity. Evidence that the AT1A receptor activates transcription factor-Stat91 and/or a related protein. *J Biol Chem* 269: 31443–31449, 1994.
3. **Booz GW, Conrad KM, Hess AL, Singer HA, Baker KM.** Angiotensin-II-binding sites on hepatocyte nuclei. *Endocrinology* 130: 3641–3649, 1992.
4. **Camargo de Andrade MC, Di Marco GS, de Paulo Castro Teixeira V, Mortara RA, Sabatini RA, Pesquero JB, Boim MA, Carmona AK, Schor N, Casarini DE.** Expression and localization of N-domain ANG I-converting enzymes in mesangial cells in culture from spontaneously hypertensive rats. *Am J Physiol Renal Physiol* 290: F364–F375, 2006.
5. **Chen R, Mukhin YV, Garnovskaya MN, Thielin TE, Iijima Y, Huang C, Raymond JR, Ullian ME, Paul RV.** A functional angiotensin II receptor-GFP fusion protein: evidence form agonist-dependent nuclear translocation. *Am J Physiol Renal Physiol* 279: F440–F448, 2000.
6. **Derbyshire ZE, Halfter UM, Heimark RL, Sy TH, Vaillancourt RR.** Angiotensin II stimulated transcription of cyclooxygenase II is regulated by a novel kinase cascade involving Pyk2, MEKK4 and annexin II. *Mol Cell Biochem* 271: 77–90, 2005.
7. **Dingwall C, Laskey RA.** Nuclear targeting sequences–a consensus? *Trends Biochem Sci* 16: 478–481, 1992.
8. **Duff JL, Marrero MB, Paxton WG, Schieffer B, Bernstein KE, Berk BC.** Angiotensin II signal transduction and the mitogen-activated protein kinase pathway. *Cardiovasc Res* 30: 511–517, 1995.
9. **Eggena P, Zhu JH, Clegg K, Barrett JD.** Nuclear angiotensin receptors induce transcription of renin and angiotensinogen mRNA. *Hypertension* 22: 496–501, 1993.
10. **Eggena P, Zhu JH, Sereevinyayut S, Giordani M, Clegg K, Andersen PC, Hyun P, Barrett JD.** Hepatic angiotensin II nuclear receptors and transcription of growth-related factors. *J Hypertens* 14: 961–968, 1996.
11. **Filipeanu CM, Brailoiu E, Kok JW, Henning RH, De Zeeuw D, Nelemans SA.** Intracellular angiotensin II elicits Ca^{2+} increases in A7r5 vascular smooth muscle cells. *Eur J Pharmacol* 420: 9–18, 2001.
12. **Filipeanu CM, Henning RH, de Zeeuw D, Nelemans A.** Intracellular angiotensin II and cell growth of vascular smooth muscle cells. *Br J Pharmacol* 132: 1590–1596, 2001.
13. **Gaborik Z, Jagadeesh G, Zhang M, Spat A, Catt KJ, Hunyady L.** The role of a conserved region of the second intracellular loop in AT1 angiotensin receptor activation and signaling. *Endocrinology* 144: 2220–2228, 2003.
14. **Gaborik Z, Szaszak M, Szidonya L, Balla B, Paku S, Catt KJ, Clark AJL, Hunyady L.** β-Arrestin- and dynamin-dependent endocytosis of the AT1 angiotensin receptor. *Mol Pharmacol* 59: 239–247, 2001.
15. **Gashler A, Sukhatme VP.** Early growth response protein 1 (Egr-1): prototype of a zinc-finger family of transcription factors. *Prog Nucleic Acid Res Mol Biol* 50: 191–224, 1995.
16. **Gasparo MD, Catt KJ, Inagami T, Wright JW, Unger T.** International Union of Pharmacology. XXIII. The angiotensin II receptors. *Pharmacol Rev* 52: 415–472, 2000.
17. **Guillemot L, Levy A, Raymondjean M, Rothhut B.** Angiotensin II-induced transcriptional activation of the cyclin D1 gene is mediated by Egr-1 in CHO-AT_{1A} cells. *J Biol Chem* 276: 39394–39403, 2001.
18. **Haendeler J, Berk BC.** Angiotensin II mediated signal transduction. Important role of tyrosine kinases. *Regul Pept* 95: 1–7, 2000.
19. **Haller H, Lindschau C, Quass P, Luft FC.** Intracellular actions of angiotensin II in vascular smooth muscle cells. *J Am Soc Nephrol* 10: S75–S83, 1999.
20. **Hodel MR, Corbett AH, Hodel AE.** Dissection of a nuclear localization signal. *J Biol Chem* 276: 1317–1325, 2001.
21. **Hu ZW, Kerb R, Shi XY, Wei-Lavery T, Hoffman BB.** Angiotensin II increases expression of cyclooxygenase-2: implications for the function of vascular smooth muscle cells. *J Pharmacol Exp Ther* 303: 563–573, 2002.
22. **Hunyady L, Bor M, Balla T, Catt KJ.** Identification of a cytoplasmic Ser-Thr-Leu motif that determines agonist-induced internalization of the AT_1 angiotensin receptor. *J Biol Chem* 269: 31378–31382, 1994.
23. **Hunyady L, Bor M, Baukal AJ, Balla T, Catt KJ.** A conserved NPLFY sequence contributes to agonist binding and signal transduction but is not an internalization signal for the type 1 angiotensin II receptor. *J Biol Chem* 270: 16602–16609, 1995.

24. **Kang J, Shi Y, Xiang B, Qu B, Su W, Zhu M, Zhang M, Bao G, Wang F, Zhang X.** A nuclear function of β-arrestin 1 in GPCR signaling: regulation of histone acetylation and gene transcription. *Cell* 123: 833–847, 2005.
25. **Lee DK, Lanca AJ, Cheng R, Nguyen T, Ji XD, Gobeil F Jr, Chemtob S, George SR, O'Dowd BF.** Agonist-independent nuclear localization of the apelin, angiotensin AT_1, and bradykinin B_2 receptors. *J Biol Chem* 279: 7901–7908, 2004.
26. **Ling S, Dai A, Ma YH, Wilson E, Chatterjee K, Ives HE, Sudhir K.** Matrix-dependent gene expression of egr-1 and PDGF A regulate angiotensin II-induced proliferation in human vascular smooth muscle cells. *Hypertension* 34: 1141–1146, 1999.
27. **Lu D, Yang H, Shaw G, Raizada MK.** Angiotensin II-induced nuclear targeting of the angiotensin type 1 (AT1) receptor in brain neurons. *Endocrinology* 139: 365–375, 1998.
28. **Luttrell LM, Roudabush FL, Choy EW, Miller WE, Field ME, Pierce KL, Lefkowitz RJ.** Activation and targeting of extracellular signal-regulated kinases by β-arrestin scaffolds. *Proc Natl Acad Sci USA* 98: 2449–2454, 2001.
29. **Makkerh JP, Dingwall C, Laskey RA.** Comparative mutagenesis of nuclear localization signals reveals the importance of neutral and acidic amino acids. *Curr Biol* 6: 1025–1027, 1996.
30. **Marrero MB, Schieffer B, Paxton WG, Heerdt L, Berk BC, Delafontaine P, Bernstein KE.** Direct stimulation of Jak/STAT pathway by the angiotensin II receptor. *Nature* 375: 247–250, 1995.
31. **Ohnaka K, Numaguchi K, Yamakawa T, Inagami T.** Induction of cyclooxygenase-2 by angiotensin II in cultured rat vascular smooth muscle cells. *Hypertension* 35: 68–75, 2000.
32. **Pokholok DK, Zeitlinger J, Hannett NM, Reynolds DB, Young RA.** Activated signal transduction kinases frequently occupy target genes. *Science* 313: 533–536, 2006.
33. **Re R, Parab M.** Effect of angiotensin II on RNA synthesis by isolated nuclei. *Life Sci* 34: 647–651, 1984.
34. **Re RN, LaBiche RA, Bryan SE.** Nuclear hormone mediated changes in chromatin solubility. *Biochem Biophys Res Commun* 110: 61–68, 1983.
35. **Robbins J, Dilworth SM, Laskey RA, Dingwall C.** Two interdependent basic domains in nucleoplasmin nuclear targeting sequence: identification of a class of bipartite nuclear targeting sequence. *Cell* 64: 615–623, 1991.
36. **Seta K, Nanamori M, Modrall JG, Neubig RR, Sadoshima J.** AT1 receptor mutant lacking heterotrimeric G protein coupling activates the Src-Ras-ERK pathway without nuclear translocation of ERKs. *J Biol Chem* 277: 9268–9277, 2002.
37. **Shamim A, Pelzer T, Grohe C, Neyses L.** Induction of Egr-1 mRNA and protein by endothelin 1, angiotensin II and norepinephrine in neonatal cardiac myocytes. *Mol Cell Biochem* 195: 11–17, 1999.
38. **Simmons DL, Botting RM, Hla T.** Cyclooxygenase isozymes: the biology of prostaglandin synthesis and inhibition. *Pharmacol Rev* 56: 387–437, 2004.
39. **Simone C, Forcales SV, Hill DA, Imbalzano AN, Latella L, Puri PL.** p38 pathway targets SWI-SNF chromatin-remodeling complex to muscle-specific loci. *Nat Genet* 36: 738–743, 2004.
40. **Smith RD, Hunyady L, Olivares-Reyes JA, Mihalik B, Jayadev S, Catt KJ.** Agonist-induced phosphorylation of the angiotensin AT1a receptor is localized to a serine/threonine-rich region of its cytoplasmic tail. *Mol Pharmacol* 54: 935–941, 1998.
41. **Tang SS, Rogg H, Schumacher R, Dzau VJ.** Characterization of nuclear angiotensin-II-binding sites in rat liver and comparison with plasma membrane receptors. *Endocrinology* 131: 374–380, 1992.
42. **Thomas WG, Baker KM, Motel TJ, Thekkumkara TJ.** Angiotensin II receptor endocytosis involves two distinct regions of the cytoplasmic tail: a role for residues on the hydrophobic face of a putative amphipathic helix. *J Biol Chem* 270: 22153–22159, 1995.
43. **Touyz RM, Schiffrin EL.** Signal transduction mechanisms mediating the physiological and pathophysiological actions of angiotensin II in vascular smooth muscle cells. *Pharmacol Rev* 52: 639–672, 2000.
44. **Turner NA, Ball SG, Balmforth AJ.** The mechanism of angiotensin II-induced extracellular signal-regulated kinase-1/2 activation is independent of angiotensin AT1A receptor internalisation. *Cell Signal* 269: 269–277, 2001.
45. **Zhang J, Ferguson SSG, Barak LS, Menard L, Caron MG.** Dynamin and β-arrestin reveal distinct mechanisms for G protein-coupled receptor internalization. *J Biol Chem* 271: 18302–18305, 1996.